

# **POWER GENERATION OF MILLIMETER-WAVE SiC AVALANCHE TRANSIT TIME OSCILLATOR AT HIGH TEMPERATURE**

**C. C. Meng and G. Z. Liao**

**Department of Electrical Engineering  
National Chung-Hsing University  
Taichung, Taiwan, Republic of China**

## **ABSTRACT**

For the first time, millimeter-wave SiC (Silicon Carbide) IMPATT oscillator was analyzed at 500 K and 800 K with temperature dependent ionization rates and saturation velocity. The large signal simulations demonstrate the fact that SiC IMPATT devices have efficiency and power advantage over Si and GaAs IMPATT devices at millimeter-wave frequencies. The efficiencies (and d.c. power density) at 800 K for depletion widths of 0.25  $\mu$ m (200 GHz), 0.5  $\mu$ m (100 GHz) and 1  $\mu$ m (50 GHz) are 12.4% (6.7 MW/cm<sup>2</sup>), 15% (4.5 MW/cm<sup>2</sup>) and 15.8% (3.3 MW/cm<sup>2</sup>), respectively, for p<sup>+</sup>n single-drift flat-profile structures.

## **INTRODUCTION**

SiC material, due to its superior electronic and thermal properties, has been recognized as an excellent candidate for millimeter-wave IMPATT oscillator. The high breakdown electric fields of 4X10<sup>6</sup> V/cm and high saturation velocity of 2X10<sup>7</sup> cm/s (room temperature) result in the d.c. power density of SiC IMPATT oscillator about 50 times higher than Si and GaAs IMPATT oscillators. Tremendous heat generated can be

dissipated away because SiC material has excellent thermal conductivity of 4.9 W/cm-K and the SiC IMPATT device can be operated at 800 K due to its wider bandgap, 3 eV [1], [2].

## **IMPACT IONIZATION RATES AT HIGH TEMPERATURE**

The millimeter-wave SiC IMPATT device operates at high temperature and over very high electric fields. A knowledge of ionization rates as a function of the electric fields at high temperature is, thus, needed in the large signal simulation. In this paper, a lucky drift model is used to extrapolate the experimental data at high electric fields and high temperature[3] because almost all the available experimental data were measured at room temperature and lower electric fields[1]. The lucky drift model describes the ionization rates as a function of electric fields and temperature by four physical parameters- momentum relaxation length at zero Kevin ( $\lambda_{m0}$ ), ionization mean free length at zero Kevin, ( $\lambda_{ion0}$ ), phonon energy ( $E_p$ ) and ionization threshold energy ( $E_T$ ). These four physical parameters are independent of electric field and temperature. When  $E_p=109$  meV,  $E_T=4$  eV for electrons and  $E_T=3$  eV for holes were chosen to fit the experimental data,  $\lambda_{m0}=21.7$  symbol 143 \f "LotusLineDraw" \s 14 }  $\lambda_{ion0}=180$ symbol 143 \f "LotusLineDraw" \s 14 } for electrons and  $\lambda_{m0}=19.1$ symbol 143 \f "LotusLineDraw" \s 14 }  $\lambda_{ion0}=125$ symbol 143 \f "LotusLineDraw" \s 14 } for holes were obtained.

## LARGE SIGNAL SIMULATION

Many full scale simulation schemes for IMPATT devices are described in the literature and accurate results can be obtained provided that precise physical parameters are given[4]. Sometimes room temperature saturation velocity and ionization rates are used in the full scale simulation because the lack of high temperature experimental data. On the other hand, a Read type analysis, which has well-defined avalanche and drift regions, can provide more physical insights and is sufficient to understand at what frequency efficiency falls off[5]. In this paper, a Read type large signal simulation[3] is used to analyze the efficiency of millimeter-wave SiC IMPATT oscillators at high temperature (800 K and 500K). The normalized d.c. current density is set to 0.1 for all the simulations.

Efficiency can be calculated as a function of r.f. voltage amplitude for a given depletion width because a prior knowledge of the carrier's saturation velocity is not needed in this simulations when the transit angle is set to  $\pi$ . Figure 1 and figure 2 illustrates the efficiency vs. amplitude modulation for SiC single-drift flat-profile for different depletion widths at 800 K and 500 K, respectively. In figure 1 and figure 2, Values in parentheses are proportional to the electron saturation velocity and a saturation velocity of  $10^7$  cm/s for electrons is assumed for both 500 K and 800 K to obtain the corresponding frequencies. The value is a factor of two reduction from its room temperature value. If a different saturation velocity is assumed, the efficiency is the same for a given depletion width and only a re-normalization for the corresponding frequency is needed.

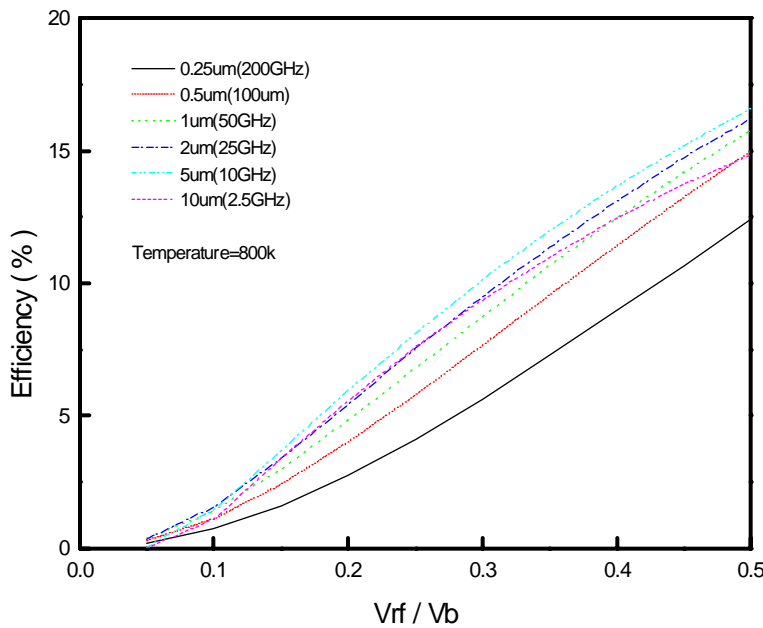


Fig.1 Efficiency as a function of modulation for SiC IMPATT device at 800K.

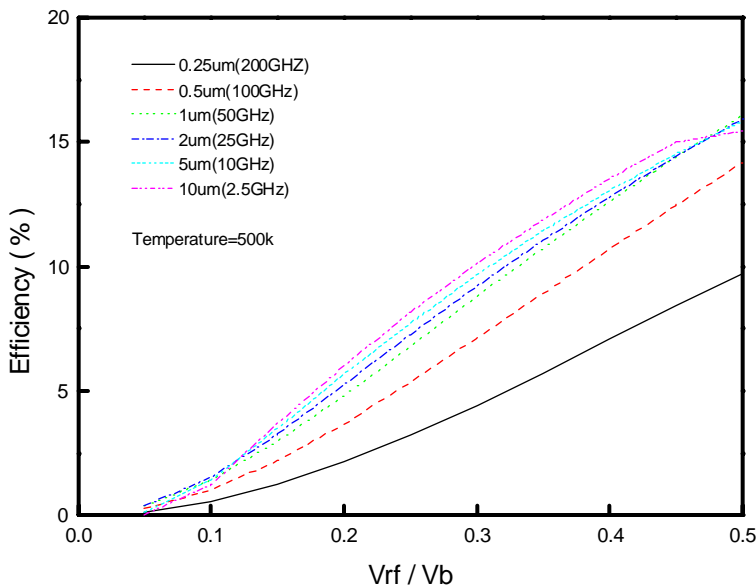


Fig.2 Efficiency as a function of modulation for SiC IMPATT device at 500K.

Figure 3 illustrates efficiency as a function of frequencies at 800K and 500K for 50% amplitude modulation. Efficiency starts to fall off for frequencies above 100 GHz. Even so, the efficiency of a SiC IMPATT single-drift flat-profile device below 50 GHz is comparable to the Si and GaAs single-drift flat-profile IMPATT device and outperforms the Si and GaAs IMPATT devices for the frequencies above 50 GHz.

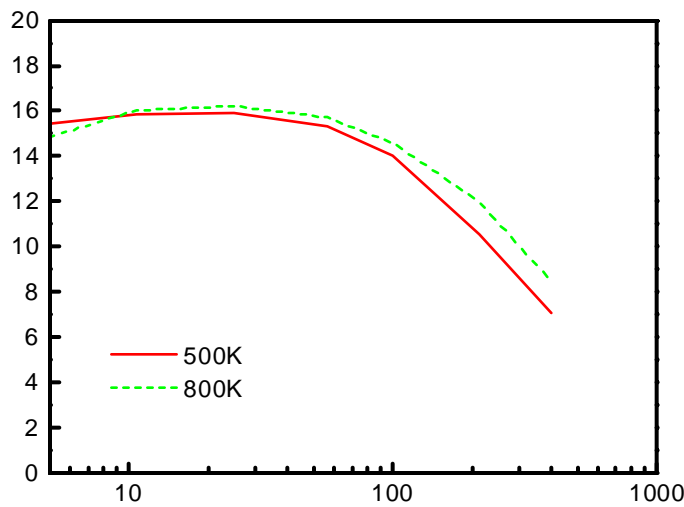


Fig.3 Efficiency as a function of frequency for SiC IMPATT device at 800K and 500K when  $V_{rf}/V_b = 0.5$

The efficiency fall-off for the frequencies above 100 GHz comes from the reduction of nonlinearity in the avalanche process when the IMPATT device is biased at higher electric fields for higher frequency operation. Figure 4 illustrates the normalized injection current and normalized induced current for SiC IMPATT devices with depletion width of 0.125  $\mu\text{m}$  (400 GHz) and 1  $\mu\text{m}$  (50 GHz) at 800 K. The amplitude modulation is 50%. Figure 5 differes from figure 4 only at the temperature,

500 K instead of 800 K. The strong nonlinearity in the avalanche process leads to a sharp avalanche current pulse and a square-like induced current pulse; while saturation of ionization rates at higher electrical fields results in a broaden avalanche injection current pulse and sinusoidal-like induced current as shown in figure 4 and figure 5. The efficiencies (and d.c. power density) at 800 K for depletion widths of 0.25  $\mu\text{m}$  (200 GHz), 0.5  $\mu\text{m}$  (100 GHz) and 1  $\mu\text{m}$  (50 GHz) are 12.4% (6.7 MW/cm $^2$ ), 15% (4.5 MW/cm $^2$ ) and 15.8% (3.3 MW/cm $^2$ ), respectively. The efficiency (and d.c. power density) at 500 K for depletion widths of 0.25  $\mu\text{m}$  (200 GHz), 0.5  $\mu\text{m}$  (100 GHz) and 1  $\mu\text{m}$  (50 GHz) are 9.8% (5.4 MW/cm $^2$ ), 14.2% (3.7 MW/cm $^2$ ) and 16.1% (2.7 MW/cm $^2$ ), respectively, for p $^+$ n single-drift flat-profile structures.

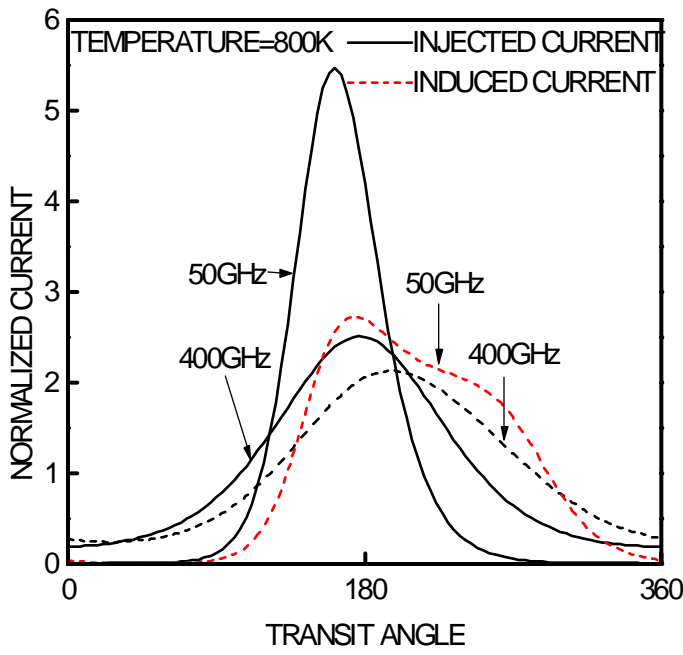


Fig.4 Injected and induced current waveform for 1  $\mu\text{m}$  (50 GHz) and 0.125  $\mu\text{m}$  (400 GHz) SiC IMPATT device at 800 K when  $V_{rf}/V_b=0.5$ .

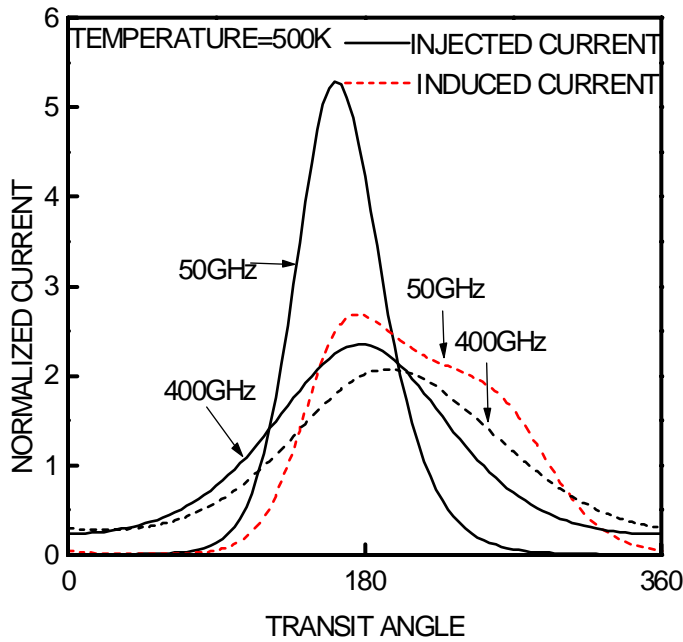


Fig.5 Injected and induced current waveform for  $1\mu\text{m}$  (50GHz) and  $0.125\mu\text{m}$  (400GHz) SiC IMPATT device at 500K when  $V_{rf}/V_b=0.5$

The normalized admittances for a SiC IMPATT device with  $0.125\mu\text{m}$  (400 GHz),  $1\mu\text{m}$  (50 GHz) at 800 K are plotted in figure 6. The value for transit angle varies from  $0.75\pi$  to  $1.5\pi$  in  $0.25\pi$  intervals and the normalized r.f. amplitude varies from 0.1 to 0.5 in 0.1 (or 0.2) intervals. The larger conductance at lower frequency comes from the increase in the nonlinearity of the avalanche process, while the susceptance mainly comes from the cold capacitance. The decrease in quality factor at lower frequency facilitates the impedance matching to the oscillator circuit and the resulting device is less susceptible to the series resistance.

## **DISCUSSION AND CONCLUSION**

The simulations analyzed the millimeter-wave SiC IMPATT devices at high temperature. A Read type analysis is less accurate at the efficiency fall-off frequencies because saturation of ionization rates occurs. There is no well-defined avalanche region at the efficiency fall-off frequencies. Thus, a full scale simulation is needed for better accuracy. Nonetheless, a Read type analysis is sufficient to predict at what frequency the efficiency falls off. The efficiency remains high at the frequency below 200 GHz for a single-drift flat-profile structure. Thus, for frequencies below 200 GHz, it is feasible to design a hi-low or low-hi-low Read types structure to further optimize the efficiency by reducing the voltage drop at the avalanche region. The out power and efficiency can be further improved by using a double-drift type design. In conclusion, millimeter-wave SiC IMPATT device was analyzed at high temperature with temperature dependent ionization rates and saturation velocity for the first time. Our simulation confirms the efficiency and power advantage of millimeter-wave SiC IMPATT devices.

## **ACKNOWLEDGMENT**

This work was supported by the National Science Council of Republic of China under the contract number NSC 86-2221-E-005-012.

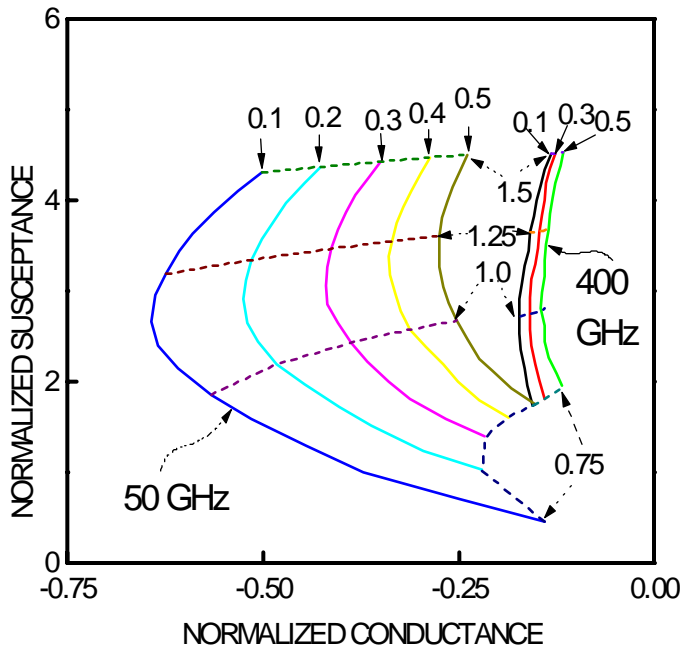


Fig.6 Normalized conductance and susceptance for  $1\mu\text{m}$  (50GHz) and  $0.125\mu\text{m}$  (400GHz) SiC IMPATT device at 800K . Solid arrows point to the normalized r.f. voltage amplitudes and dash arrows point to the nomalized frequencies.

## REFERENCES

- [1] M. Ruff, H. Mitlehner, and R. Helbig, “SiC devices: physics and numerical simulation,” *IEEE Trans. Electron Devices*, Vol. ED-41, p.1040, 1994 and references therein.
- [2] C. E. Weitzel, J. W. Palmour, C. H. Carter, Jr., K. Moore, K. J. Nordquist, S. Allen, C. Thero and M. Bhatnagar, “Silicon carbide high-power devices,” *IEEE Trans. Electron Devices*, Vol. ED-43, p.1732, 1996.

[3] C. C. Meng and H. R. Fetterman, “A theoretical analysis of millimeter-wave GaAs/AlGaAs multiquantum well transit time devices by the lucky drift model,” *Solid-State Electron.*, Vol. 36 p.435, 1993.

[4] I. Mehdi, G. I. Haddad and R. K. Mains, “Microwave and millimeter-wave power generation in silicon carbide avalanche devices,” *J. Appl. Phys.* 64(3), p.1533, 1988.

[5] T. Misawa, “High-frequency fall-off of IMPATT diode efficiency,” *Solid-State Electron.*, Vol. 15, p.457, 1972.